Published in final edited form as:
Circulation. 2006 February 28; 113(8): 1101–1107.

Real-Time MRI-Guided Endovascular Recanalization of Chronic Total Arterial Occlusion in a Swine Model

Amish N. Raval, MD, **Parag V. Karmarkar, MSc**, **Michael A. Guttman, MSc**, **Cengizhan Ozturk, MD, PhD**, **Smita Sampath, PhD**, **Ranil DeSilva, MBBS, PhD**, **Ronnier J. Aviles, MD**, **Minnan Xu, BS**, **Victor J. Wright, BS**, **William H. Schenke, BS**, **Ozgur Kocaturk, MSc**, **Alexander J. Dick, MD**, **Venkatesh K. Raman, MD**, **Ergin Atalar, PhD**, **Elliot R. McVeigh, PhD**, and **Robert J. Lederman, MD**

From the Cardiovascular Branch (ANR, PVK, CO, RDS, RJA, VJW, WHS, OK, AJD, VKR, RJL) and the Laboratory of Cardiac Energetics (MAG, SS, ERM), Division of Intramural Research, National Heart Lung and Blood Institute, National Institutes of Health, Bethesda, MD, USA; Cardiovascular Section, Department of Medicine, University of Wisconsin, Madison, WI, USA (ANR); Department of Radiology (PVK, MX, EA), The Johns Hopkins University, Baltimore, MD, USA

Abstract

Background—Endovascular recanalization (guidewire traversal) of peripheral artery chronic total occlusion (CTO) can be challenging. X-Ray angiography resolves CTO poorly. Virtually “blind” device advancement during X-ray-guided interventions can lead to procedure failure, perforation and hemorrhage. Alternatively, magnetic resonance imaging (MRI) may delineate the artery within the occluded segment to enhance procedural safety and success. We hypothesized that real-time MRI (rtMRI) guided CTO recanalization can be accomplished in an animal model.

Methods and Results—Carotid artery CTO was created by balloon injury in 19 lipid overfed swine. After 6–8 weeks, two underwent direct necropsy analysis for histology, three underwent primary X-ray-guided CTO recanalization attempts, and the remaining 14 underwent rtMRI-guided recanalization attempts in a 1.5T interventional MRI system. rtMRI intervention used custom CTO catheters and guidewires that incorporated MRI receiver antennae to enhance device visibility.

The mean length of the occluded segments was 13.3 ± 1.6cm. rtMRI-guided CTO recanalization was successful in 11/14 swine and only 1/3 swine using X-ray alone. After unsuccessful rtMRI (n = 3), X-ray-guided attempts also were all unsuccessful.

Conclusions—Recanalization of long CTO is feasible entirely using rtMRI guidance. Low profile clinical-grade devices will be required to translate this experience to humans.

Endovascular recanalization of chronic total arterial occlusion (CTO) is challenging under conventional X-ray guidance because devices are advanced almost blindly. MRI can image CTO borders and luminal contents, and could potentially guide these procedures. We test the feasibility of real-time MRI guided wire traversal in a swine model of peripheral artery CTO using custom active MRI catheters.

Address for Correspondence: Robert J. Lederman, MD, Cardiovascular Branch, Division of Intramural Research, National Heart, Lung, and Blood Institute, National Institutes of Health, Building 10, Room 2c713, MSC 1538, Bethesda, MD 20892-1538, USA. Telephone: 1-301-402-6769. Email: lederman@nih.gov.

Journal Subject Head for Circulation
[23] Endovascular coronary and valvular interventions: other
[58] Computerized tomography and Magnetic Resonance Imaging
[130] Animal models of human disease

Conflicts of Interest Disclosures
None.

MESH-related Keywords

Real-time magnetic resonance imaging; Interventional MRI; Magnetic Resonance Imaging/methods

Background

Chronic total occlusion (CTO) of peripheral arteries can cause disabling intermittent claudication or critical limb ischemia. Surgical revascularization offers symptom relief and limb salvage in eligible patients; however, perioperative morbidity, lengthy hospital stay and slow functional recovery limit wider application[1, 2]. Endovascular techniques are appealing because they offer prompt return of function and require neither general anesthesia nor extended hospital stay. However, endovascular recanalization of long, tortuous, occluded peripheral arteries remains challenging and risky, and thus, surgical or conservative management are typically recommended[1].

X-Ray fluoroscopic angiography with radiocontrast identifies the occluded inflow artery and possibly collateral-dependent outflow beyond the occlusion, but cannot discriminate CTO arterial wall and lumen. In these cases, the entire occluded arterial segment remains invisible to the operator. Virtually “blind” device manipulation risks procedural failure and arterial perforation. Furthermore, ionizing radiation and nephrotoxic contrast exposure may become excessive during lengthy CTO recanalization procedures.

Magnetic resonance imaging (MRI) can image the entire peripheral artery occlusion including arterial wall, lumen content, and adjacent structures, without ionizing radiation or iodinated radiocontrast. Advances in rapid imaging, combined with development of catheter devices visible under MRI, have made real-time MRI (rtMRI) guided therapeutic interventions feasible[3–19]. We hypothesize that rtMRI can guide catheter navigation within an occluded artery, and that combined CTO recanalization and percutaneous transluminal angioplasty can be conducted entirely under rtMRI guidance using custom MRI-visible devices in a swine model.

Methods

Balloon Injury Model

Animal protocols were approved by the National Heart, Lung, and Blood Institute Animal Care and Use Committee. NIH mini-swine (mean weight, 50 ± 12 kg) were fed 2% high cholesterol diet for 1 week prior to CTO model creation, and thereafter until recanalization was attempted 6 to 8 weeks later. After transfemoral access, an angioplasty balloon (*Agiltrac*, Guidant) sized 1.5 to 2 times artery diameter was positioned in the mid left carotid artery (LCA), inflated to nominal pressure, and rapidly withdrawn up to six times. Contrast-enhanced magnetic resonance angiography (CEMRA) was performed at 2 weeks to confirm CTO. If the LCA remained patent (n = 4), balloon injury was repeated.

Histology was performed on two uninstrumented CTO arteries, 8 weeks after balloon injury. Formalin fixed, paraffin embedded, transverse sections (4 μm) were taken at 5 mm intervals along the artery length, and stained with Hematoxylin and Eosin and Masson’s Trichrome.

Interventional MRI Suite

Procedures were performed in a previously described combined X-ray-MRI interventional suite (*Axiom Artis*/1.5T *Sonata*, Siemens) [20]. In-room hemodynamics, scan control and rendered images were displayed using shielded LCD projectors. Optical microphones (Phone-Or) and filtered headsets (Magnacoustics) permitted staff communication.

Digital subtraction X-ray and CEMRA of the arch and great vessels were performed immediately before and after intervention. Typical parameters [TR = repetitition time (ms) / TE = echo time (ms) /FA = flip angle (degrees) /BW = bandwidth (Hz/per pixel) /VOX = voxel size (mm)]: [TR/TE/FA/BW/VOX = 3.7/1.4/25/375/0.3x0.5x2, slab 300x244x128mm]. Real-time steady state free precession (rtSSFP) and 2D T1 weighted (T1w) spin echo axial images representing key anatomic planes were stored for uninterrupted retrieval during the intervention. Typical parameters:[rtSSFP: TR/TE/FA/BW/VOX = 3.5/1.7/45/975/1.0x1.4x4] and [T1w:TR/TE/FA/BW/VOX = 800/12/180/130/0.5x0.5x3, 2 averages].

During rapid device manipulation in the aortic arch, rtSSFP frame rate was accelerated 3:1 using echo-sharing wherein image data are interleaved over adjacent frames. Saturation pre-pulses suppressed background tissue to better visualize inflation of balloons filled with gadopentate dimeglumine (0.8% Gd-DTPA, *Magnevist*, Berlex) and of selective intra-arterial angiography (2.4% Gd-DTPA). Uninterrupted real-time subtraction angiography was achieved by displaying the difference between maximum intensity projections in time before and after the injection. Voxel size was reduced to increase spatial resolution, and temporal image filtering (averaging) was applied to improve signal-to-noise ratio (SNR) during slow device advancement within the CTO. Multiple oblique slices could be acquired simultaneously, repositioned interactively and individually disabled and enabled as desired. Custom scan features allowed adjustment of pulse sequence, reconstruction and display parameters without scan interruption. Finally, signals from separate device antennae could be independently displayed along their entire length, color-highlighted and combined in real-time with anatomic images from surface coils.

Interventional Devices

Active devices were prepared and tested in our laboratory. The intent was to create devices that were conspicuous along their entire length, including the tip.

Custom MRI active CTO support catheter—Distal 1cm microcoils were mounted on 6Fx100cm angled, tapered, custom tungsten-braided catheters (Minnesota MedTec). Coil signals are transmitted along the catheter shaft under insulating polyimide. Tuning, matching and decoupling circuitry were attached at the proximal hub, in order to prevent heating during MRI. The device was connected to a separate MR scanner receiver channel, so that device-related images could be displayed in color.

Custom MRI active CTO guidewire: (Figure 1)—Consecutive gold-silver-gold-plated nitinol core wires were inserted within nitinol hypotubes, separated by polymer insulation. Closely wound MP35N (cobalt-chromium alloy) microcoils were attached distally to add wire flexibility, and 2.5cm distal microcoils enhanced MRI receiver sensitivity at the tip. The final receiver-coil guidewire was 0.032” x 155cm, straight, and stiff. The proximal end of the guidewire had detachable connectors permitting catheter exchange.

Custom active flexible “workhorse” guidewire—Flexible tip nitinol guidewires (*Nitrex*, ev3, 0.032” x 155 cm) were altered to serve as active, “loopless” design[21] receiver coils that were visible along their entire length. These were used as “workhorse” wires to safely deliver the CTO catheter to the origin of the occluded carotid artery.

Delivery Sheath—10F delivery sheaths (*Fast Cath*, St. Jude; *Brite Tip*, Cordis) were trimmed to 75cm. Stainless steel MRI markers (1mm x 0.014 inch) were bonded to the sheath tip creating passive markers (discrete signal void) during MRI.

Device Testing—MRI heating tests (Appendix) were performed on CTO support catheters and guidewires using previously described methods[22, 23].

rtMRI-Guided CTO recanalization

The primary study endpoint was successful traversal of occluded arteries from their patent origins to their patent outflow regions. The secondary study endpoint was restoration of antegrade flow by adjunctive balloon angioplasty.

Animals were pretreated with aspirin 325 mg and clopidogrel 300mg. Intravenous heparin 100U/kg bolus was given initially and supplemented with 50U/kg every 2 hours. Following sheath insertion, the active CTO support catheter was navigated to the brachiocephalic artery over the active floppy guidewire and positioned proximal to the occluded LCA. The floppy wire was exchanged for the active CTO wire. The CTO guidewire and catheter were steered intraluminally through the CTO, using multi-slice rtMRI. Two parallel slices orthogonal to the CTO artery centerline were used to ensure an intraluminal device course. One slice tracked the wire tip, and the second advanced ahead of the wire tip providing a target for the operator. Once the CTO was traversed, a 260cm PTFE guidewire (*Glidewire*, Terumo) was used to exchange the CTO guide catheter for a 100mm long peripheral angioplasty balloon sized 1:1 to the artery wall. Following several balloon inflations with 5mM Gd-DTPA, selective angiography was performed using 5mL of 10mM Gd-DTPA. Intra-arterial nitroglycerin 200–400mcg was administered as needed to treat spasm.

Comparative X-ray-guided Recanalization of CTO model

X-ray guided recanalization was attempted in three swine, by experienced interventionists to assess the suitability and procedural difficulty of the CTO model. Contemporary techniques and devices were used (*Shinobi* 0.014”, Cordis; *Cross-It* 0.010–0.014”, Guidant; *Glidewire* Straight Stiff and Super-Stiff 0.035”; 4F *Glidecath*, Terumo). Each attempt used high-performance, X-ray imaging (*Artis FC*, Siemens) with 13cm field of view, 15fps, appropriate collimation, and at least 60 minutes of fluoroscopy. In three additional swine, after unsuccessful MRI-guided recanalization, X-ray-guided recanalization also was attempted.

Statistics and Analysis

Continuous variables were reported as mean ± standard deviation and were compared using a two-tailed Student’s t-test (*Excel 2003*, Microsoft). Discrete variables (procedure success) were compared using Fisher’s exact test[24]. The authors had full access to the data and take responsibility for its integrity. All authors have read and agree to the manuscript as written.

Results

Device Heating Tests

No significant heating was observed in phantom experiments during MRI of active CTO support catheters and guidewires (Appendix).

CTO Model Geometry and Histopathology

Native LCA diameter by X-ray was 4.6 ± 0.7mm before balloon injury, measured 70mm cranial to the carotid bifurcation. Immediate pre-intervention CTO diameter (T1w) at this level, and CTO length (CEMRA) were 4.7 ± 1.3mm and 133 ± 16mm. By comparison, the contralateral carotid artery diameter (T1w) at this level, the CTO minimal luminal diameter(T1w) and CTO maximal external wall diameter(T1w) were 5.0 ± 0.7mm, 3.1 ± 1.3mm, and 6.7 ± 1.2mm respectively. These measurements suggest zones of positive (outward) and negative (inward) remodeling in this swine CTO model and are consistent with histology. MRI identified the

entire CTO artery wall endoluminal and external boundaries, and occasional proximal dissection flaps resulting from initial balloon injury (Figure 2). Histology of the explanted, naïve CTO arteries revealed dense luminal collagen deposition, disrupted intima, microchannels and distal organized thrombus (Figure 3).

rtMRI-guided Recanalization

The primary endpoint, rtMRI-guided CTO recanalization, was achieved in 11/14 animals. The shaft profile and tips of the active devices were conspicuous while navigating the aorta and brachiocephalic arteries (Figure 4). The occluded artery walls and active interventional devices were easily visualized under MRI (Figure 5). Multi-planar imaging facilitated continuous assessment of device-anatomic relationships enabling intraluminal device traversal. Mean time to wire traversal was 55 ± 22 min (spread 25–99 min), with an observed learning curve between the first and last third of interventions performed (69 ± 23 min vs. 34 ± 7 min, $p = 0.048$). After balloon angioplasty, real-time selective MRA demonstrated brisk antegrade flow in 6/11 of those successfully recanalized with a guidewire (Figure 6). Gross necropsy of all successfully recanalized animals revealed mild artery thickening with no extramural hematoma (Figure 7) and appeared similar to the uninstrumented CTO lesions.

In 3/14 animals, the active guidewire would not advance beyond the proximal one-third of the occluded segment despite an apparently intraluminal trajectory. Following careful MRI interrogation to rule out any adverse sequelae such as hematoma, X-ray-guided attempts in all 3 were similarly unsuccessful.

In 2/11 successfully recanalized under rtMRI, antegrade blood flow was not achieved despite intra-arterial nitroglycerin and several prolonged balloon inflations, due to refractory recoil, spasm, and unavailability of suitable stents. Intraluminal position was confirmed by selective real-time MR and X-ray angiography through the wire port of balloons positioned distal to the lesion.

Home-made active CTO support catheters would not advance over active CTO guidewires that successfully traversed the occlusions in 3/11, preventing balloon exchange and subsequent angioplasty. In one of these three (the very first experimental animal), over-aggressive attempts at advancing the active catheter over the wire resulted in clear real-time visualization of extraluminal CTO wire exit followed by extravascular hematoma accumulation. This complication was immediately recognized in rtMRI, and the procedure was aborted.

Comparative X-ray-guided Recanalization

Primary X-ray guided CTO recanalization was successful in only one of 3 different animals attempted (requiring 45min of fluoroscopy time). Cross-over X-ray recanalization was also attempted in 3/14 animals in after unsuccessful recanalization under rtMRI; none were successful. Combining these, 1/6 X-ray guided procedures were successful.

Successful CTO recanalization was more likely (79% vs. 17%, $p = 0.02$) during rtMRI attempts (11/14) compared with all X-ray-guided attempts (1/6). During extended primary X-ray recanalization attempts, wire exit caused contrast extravasation in one animal, and dissection was associated with lethal mediastinal hematoma in another.

Real-time MRI enhancements

Subtraction real-time MR angiography improved visibility of intra-arterial Gd-DTPA injections compared with saturation preparation alone (Figure 6E and F). We increased spatial resolution by reducing the voxel size but this degraded the signal-to-noise ratio (SNR). We

used temporal image filtering (averaging) to improve this reduced SNR during periods of slow device motion.

Discussion

Percutaneous peripheral artery CTO intervention can be highly challenging, time-consuming and risky. Failure rates for iliac and femoropopliteal CTO are 3–36% [25–33] and 12–25%[34, 35] respectively. Novel alternative devices and techniques have had varied success for coronary and peripheral artery CTO recanalization, though to date none have prevailed clinically[7, 36–43].

This experience demonstrates successful wholly rtMRI-guided endovascular recanalization of long and challenging CTO using custom devices, in a suitable animal model. In this model, MRI was successful in 79% of attempts using homemade devices, and in 17% of all X-ray attempts using higher-performance commercial devices.

The model CTO artery diameter and length resemble long (albeit rigid) human iliofemoral artery occlusions. These lesions would be considered TASC D or best suited for surgical rather than endovascular recanalization[1]. Unlike X-ray, MRI delineates the occluded artery walls permitting truly image guided wire navigation. Custom “active” MRI CTO devices prove conspicuous and distinct from adjacent tissues. Procedure duration declined throughout this experience due to a “learning” phenomenon.

Device conspicuity, simultaneous display of multiple real-time imaging slices, and uninterrupted interactive features contributed to procedural success. Real-time selective MRA techniques using small volumes of dilute Gd-DTPA confirmed artery patency. This work represents an advance because a broad assortment of imaging and device features are fully integrated to support complex and completely rtMRI-guided vascular interventions.

Long conductive devices may heat significantly during MRI radiofrequency excitation, and pose a safety concern. The custom “active” devices used here are appropriately tuned, matched and decoupled and do not heat during scanning in a suitable test phantom (see Appendix).

Our CTO model differs from tortuous, lipid and calcium-rich atherosclerotic human iliofemoral disease. Severe arterial recoil and spasm prevented antegrade flow (n = 2) or guiding catheter traversal (n = 3) despite successful wire recanalization. The lesions were sufficiently long and challenging for a feasibility experiment. Of note, X-ray-guided recanalization attempts were less successful, even though they employed higher-performance commercial clinical devices. Indeed, MRI-guidance offers the potential to visualize the entire occluded segment and luminal boundaries, particularly in severely tortuous lesions often found in human peripheral CTO.

This experience adds to that of other published reports of rtMRI-guided procedures that traverse anatomic boundaries such as transjugular intrahepatic portosystemic shunt (TIPS)[14, 44] and atrial transeptal puncture[16, 19]. CTO recanalization is a more complex procedure because the vascular lumen is smaller, the diseased vessels tend to be tortuous, and the risk of lethal performation is higher when manipulating catheters within the high pressure arterial system. These support the principle that MRI has potential utility to guide conventional and novel catheter-based interventions because of superior tissue visualization.

Because the SNR of proton MRI is very low, there is inadequate temporal and spatial resolution to image coronary arteries in real-time using MRI. Barring unforeseen technical breakthroughs, it is unlikely that such recanalization procedures can be conducted on occluded coronary arteries.

Limitations

The comparison of X-ray and MRI-guided recanalization attempts should be interpreted with caution because of the imbalance in the number of animals in each group, and because primary and cross-over attempts were combined for analysis.

Repeated use of recycled devices, abrupt transition points, high friction and poor mechanical responsiveness account for failure to recanalize and deliver catheter devices into the target arterial occlusion in a few animals. Our home-made devices had inferior pushability, torquability, and tip-bending performance compared with clinical X-ray devices in bench testing (data not shown). Low-profile, tapered, trackable, steerable, and hydrophilic-coated active MRI devices can be manufactured using available technology, but would have been prohibitively expensive to manufacture in the small quantities tested here. In addition, suitable stents would have treated flow-limiting artery recoil and spasm, but were not employed here. Metal alloys such as nitinol, platinum-iridium, or nickel-cobalt-chromium have less MRI susceptibility artifact compared with stainless steel. Numerous reports already have been published of experimental rtMRI-guided deployment of such devices[7, 17, 18, 45]. Nevertheless, our primary endpoint, rtMRI-guided CTO recanalization was successfully accomplished using our rudimentary device prototypes. Subsequent therapy to maintain antegrade flow and patency such as stenting could be conducted under X-ray, immediately after successful rtMRI CTO recanalization.

Conclusions

This work demonstrates the feasibility of rtMRI guidance to recanalize arterial CTO using custom “active” MRI visible devices in a suitably challenging swine model. Future image-guided human peripheral artery CTO interventions may be possible using this technology. However, clinical-grade catheter devices will be need to be manufactured to translate these findings into patients.

Clinical Perspective

Traditionally, surgical bypass is preferred over X-ray guided endovascular repair for long, tortuous CTO. Endovascular guidewire traversal under X-ray is conducted almost “blindly” through occluded vessels that are not opacified by contrast. The guidewires and catheters required to recanalize these lesions risk failure, perforation and life-threatening hemorrhage. We demonstrate successful real-time MRI-guided recanalization of a long peripheral artery CTO in a suitable pig model. Real-time MRI may offer an advantage in artery visualization during CTO traversal, while obviating ionizing radiation and nephrotoxic radiocontrast.

Acknowledgements

The authors thank Kathryn Hope, Kathy Lucas and Joni Taylor for their animal care and support. Supported by NIH Z01-HL005062-03 (RJL).

References

1. Management of peripheral arterial disease (PAD). TransAtlantic Inter-Society Consensus (TASC). Section B: intermittent claudication. J Vasc Surg Jun 2000;31(1 Part 2):S54–S134.
2. Management of peripheral arterial disease (PAD). TransAtlantic Inter-Society Consensus (TASC). Section D: chronic critical limb ischaemia. J Vasc Surg Jun 2000;31(1 Part 2):S168–288.
3. Yang X, Bolster BD Jr, Kraitchman DL, Atalar E. Intravascular MR-monitored balloon angioplasty: an in vivo feasibility study. J Vasc Interv Radiol Nov–Dec;1998 9(6):953–959. [PubMed: 9840040]
4. Guttman MA, Lederman RJ, Sorger JM, McVeigh ER. Real-time volume rendered MRI for interventional guidance. J Cardiovasc Magn Reson 2002;4(4):431–442. [PubMed: 12549231]

5. Lardo AC, McVeigh ER, Jumrussirikul P, Berger RD, Calkins H, Lima J, Halperin HR. Visualization and temporal/spatial characterization of cardiac radiofrequency ablation lesions using magnetic resonance imaging. Circulation Aug 8;2000 102(6):698–705. [PubMed: 10931812]
6. Bartels LW, Bos C, van Der Weide R, Smits HF, Bakker CJ, Viergever MA. Placement of an inferior vena cava filter in a pig guided by high-resolution MR fluoroscopy at 1.5 T. J Magn Reson Imaging Oct;2000 12(4):599–605. [PubMed: 11042643]
7. Manke C, Nitz WR, Djavidani B, Strotzer M, Lenhart M, Volk M, Feuerbach S, Link J. MR imaging-guided stent placement in iliac arterial stenoses: a feasibility study. Radiology May;2001 219(2):527–534. [PubMed: 11323483]
8. Buecker A, Spuentrup E, Grabitz R, Freudenthal F, Muehler EG, Schaeffter T, van Vaals JJ, Gunther RW. Magnetic resonance-guided placement of atrial septal closure device in animal model of patent foramen ovale. Circulation Jul 23;2002 106(4):511–515. [PubMed: 12135954]
9. Rickers C, Jerosch-Herold M, Hu X, Murthy N, Wang X, Kong H, Seethamraju RT, Weil J, Wilke NM. Magnetic resonance image-guided transcatheter closure of atrial septal defects. Circulation Jan 7;2003 107(1):132–138. [PubMed: 12515755]
10. Schalla S, Saeed M, Higgins CB, Martin A, Weber O, Moore P. Magnetic resonance--guided cardiac catheterization in a swine model of atrial septal defect. Circulation Oct 14;2003 108(15):1865–1870. [PubMed: 14517162]
11. Dick AJ, Guttman MA, Raman VK, Peters DC, Pessanha BS, Hill JM, Smith S, Scott G, McVeigh ER, Lederman RJ. Magnetic resonance fluoroscopy allows targeted delivery of mesenchymal stem cells to infarct borders in Swine. Circulation Dec 9;2003 108(23):2899–2904. [PubMed: 14656911]
12. Razavi R, Hill DL, Keevil SF, Miquel ME, Muthurangu V, Hegde S, Rhode K, Barnett M, van Vaals J, Hawkes DJ, Baker E. Cardiac catheterisation guided by MRI in children and adults with congenital heart disease. Lancet Dec 6;2003 362(9399):1877–1882. [PubMed: 14667742]
13. Kuehne T, Yilmaz S, Meinus C, Moore P, Saeed M, Weber O, Higgins CB, Blank T, Elsaesser E, Schnackenburg B, Ewert P, Lange PE, Nagel E. Magnetic resonance imaging-guided transcatheter implantation of a prosthetic valve in aortic valve position: Feasibility study in swine. J Am Coll Cardiol Dec 7;2004 44(11):2247–2249. [PubMed: 15582324]
14. Kee ST, Ganguly A, Daniel BL, Wen ZBS, Butts K, Shimikawa A, Pelc NJ, Fahrig R, Dake M. MR-guided Transjugular Intrahepatic Portosystemic Shunt Creation with Use of a Hybrid Radiography/MR System. J Vasc Interv Radiol February 2005;2005 16(2):227–234. [PubMed: 15713923]
15. Schalla S, Saeed M, Higgins CB, Weber O, Martin A, Moore P. Balloon sizing and transcatheter closure of acute atrial septal defects guided by magnetic resonance fluoroscopy: assessment and validation in a large animal model. J Magn Reson Imaging Mar;2005 21(3):204–211. [PubMed: 15723375]
16. Arepally A, Karmarkar PV, Weiss C, Rodriguez ER, Lederman RJ, Atalar E. Magnetic resonance image-guided trans-septal puncture in a swine heart. J Magn Reson Imaging Mar 18;2005 21(4):463–467. [PubMed: 15779027]
17. Raman VK, Karmarkar PV, Guttman MA, Dick AJ, Peters DC, Ozturk C, Pessanha BS, Thompson RB, Raval AN, DeSilva R, Aviles RJ, Atalar E, McVeigh ER, Lederman RJ. Real-time magnetic resonance-guided endovascular repair of experimental abdominal aortic aneurysm in swine. J Am Coll Cardiol Jun 21;2005 45(12):2069–2077. [PubMed: 15963411]
18. Raval AN, Telep JD, Guttman MA, Ozturk C, Jones M, Thompson RB, Wright VJ, Schenke WH, Desilva R, Aviles RJ, Raman VK, Slack MC, Lederman RJ. Real-Time Magnetic Resonance Imaging-Guided Stenting of Aortic Coarctation With Commercially Available Catheter Devices in Swine. *Circulation.* Jul 25 2005.
19. Raval AN, Karmarkar PV, Guttman MA, Ozturk C, DeSilva R, Wright VJ, Schenke WH, Atalar E, McVeigh ER, Lederman RJ. Real-Time MRI Guided Atrial Septal Puncture and Balloon Septostomy in Swine [In Press]. *Catheterization and cardiovascular interventions.* 2005.
20. Dick AJ, Raman VK, Raval AN, Guttman MA, Thompson RB, Ozturk C, Peters DC, Stine AM, Wright VJ, Schenke WH, Lederman RJ. Invasive human magnetic resonance imaging: feasibility during revascularization in a combined XMR suite. Catheter Cardiovasc Interv Mar;2005 64(3):265–274. [PubMed: 15736247]

21. Ocali O, Atalar E. Intravascular magnetic resonance imaging using a loopless catheter antenna. Magn Reson Med 1997;37(1):112–118. [PubMed: 8978639]
22. Atalar E. Radiofrequency safety for interventional MRI procedures(1). Acad Radiol Sep;2005 12(9): 1149–1157. [PubMed: 16112515]
23. Yeung CJ, Susil RC, Atalar E. RF safety of wires in interventional MRI: using a safety index. Magn Reson Med Jan;2002 47(1):187–193. [PubMed: 11754458]
24. Preacher K, Briggs N. Interactive Fisher's Exact Test. Available at: http://www.unc.edu/~preacher/fisher/fisher.htm
25. Johnston KW. Iliac arteries: reanalysis of results of balloon angioplasty. Radiology Jan;1993 186(1): 207–212. [PubMed: 8416566]
26. Reyes R, Maynar M, Lopera J, Ferral H, Gorriz E, Carreira J, Castaneda WR. Treatment of chronic iliac artery occlusions with guide wire recanalization and primary stent placement. J Vasc Interv Radiol Nov-Dec;1997 8(6):1049–1055. [PubMed: 9399477]
27. Uher P, Nyman U, Lindh M, Lindblad B, Ivancev K. Long-term results of stenting for chronic iliac artery occlusion. J Endovasc Ther Feb;2002 9(1):67–75. [PubMed: 11958328]
28. Steinkamp H, Werk M, Wissgott C, Settmacher U, Haufe M, Hierholzer C, Felix R. Stent placement in short unilateral iliac occlusion. Technique and 24-month results. Acta Radiol Sep;2001 42(5):508–514. [PubMed: 11552889]
29. Gupta AK, Ravimandalam K, Rao VR, Joseph S, Unni M, Rao AS, Neelkandhan KS. Total occlusion of iliac arteries: results of balloon angioplasty. Cardiovasc Intervent Radiol May–Jun;1993 16(3): 165–177. [PubMed: 8334688]
30. Carnevale FC, De Blas M, Merino S, Egana JM, Caldas JG. Percutaneous endovascular treatment of chronic iliac artery occlusion. Cardiovasc Intervent Radiol Sep–Oct;2004 27(5):447–452. [PubMed: 15184998]
31. Blum U, Gabelmann A, Redecker M, Noldge G, Dornberg W, Grosser G, Heiss W, Langer M. Percutaneous recanalization of iliac artery occlusions: results of a prospective study. Radiology Nov; 1993 189(2):536–540. [PubMed: 8210387]
32. Dyet JF, Gaines PA, Nicholson AA, Cleveland T, Cook AM, Wilkinson AR, Galloway JM, Beard J. Treatment of chronic iliac artery occlusions by means of percutaneous endovascular stent placement. J Vasc Interv Radiol May–Jun;1997 8(3):349–353. [PubMed: 9152906]
33. Vorwerk D, Guenther RW, Schurmann K, Wendt G, Peters I. Primary stent placement for chronic iliac artery occlusions: follow-up results in 103 patients. Radiology Mar;1995 194(3):745–749. [PubMed: 7862973]
34. Ashley S, Brooks SG, Gehani AA, Kester RC, Rees MR. Percutaneous laser recanalisation of femoropopliteal occlusions using continuous wave Nd-YAG laser and sapphire contact probe delivery system. Eur J Vasc Surg Jul;1994 8(4):494–501. [PubMed: 8088403]
35. Lofberg AM, Karacagil S, Ljungman C, Westman B, Bostrom A, Hellberg A, Ostholm G. Percutaneous transluminal angioplasty of the femoropopliteal arteries in limbs with chronic critical lower limb ischemia. J Vasc Surg Jul;2001 34(1):114–121. [PubMed: 11436083]
36. Perin EC, Sarmento-Leite R, Silva GV, Rogers MD, Topaz O. "Wireless" laser recanalization of chronic total coronary occlusions. J Invasive Cardiol May;2001 13(5):401–405. [PubMed: 11385157]
37. Scheinert D, Laird JR Jr, Schroder M, Steinkamp H, Balzer JO, Biamino G. Excimer laser-assisted recanalization of long, chronic superficial femoral artery occlusions. J Endovasc Ther Apr;2001 8 (2):156–166. [PubMed: 11357976]
38. Yamashita T, Kasaoka S, Son R, Gordon IL, Khan R, Neet J, Hedrick AD, Tobis JM. Optical coherent reflectometry: a new technique to guide invasive procedures. Catheter Cardiovasc Interv Oct;2001 54(2):257–263. [PubMed: 11590695]
39. Mossop P, Cincotta M, Whitbourn R. First case reports of controlled blunt microdissection for percutaneous transluminal angioplasty of chronic total occlusions in peripheral arteries. Catheter Cardiovasc Interv Jun;2003 59(2):255–258. [PubMed: 12772253]
40. Coggia M, Javerliat I, Di Centa I, Colacchio G, Leschi JP, Kitzis M, Goeau-Brissonniere OA. Total laparoscopic bypass for aortoiliac occlusive lesions: 93-case experience. Journal of Vascular Surgery 2004/11;2004 40(5):899–906. [PubMed: 15557903]

41. Casserly IP, Sachar R, Bajzer C, Yadav JS. Utility of IVUS-guided transaccess catheter in the treatment of long chronic total occlusion of the superficial femoral artery. Catheter Cardiovasc Interv Jun;2004 62(2):237–243. [PubMed: 15170719]

42. Yang YM, Mehran R, Dangas G, Reyes A, Qin J, Stone GW, Leon MB, Moses JW. Successful use of the frontrunner catheter in the treatment of instent coronary chronic total occlusions. Catheter Cardiovasc Interv Dec;2004 63(4):462–468. [PubMed: 15558776]

43. Kawarada O, Yokoi Y, Morioka N, Nakata S, Takemoto K. Chronic total occlusions in the superficial femoral artery: A novel strategy using a 1.5 mm J-tip hydrophilic guidewire with an over-the-wire balloon catheter under ultrasound guidance. Catheter Cardiovasc Interv Jun;2005 65(2):187–192. [PubMed: 15898072]

44. Kee ST, Rhee JS, Butts K, Daniel B, Pauly J, Kerr A, O'Sullivan GJ, Sze DY, Razavi MK, Semba CP, Herfkens RJ, Dake MD. 1999 Gary J. Becker Young Investigator Award. MR-guided transjugular portosystemic shunt placement in a swine model. J Vasc Interv Radiol May;1999 10(5): 529–535. [PubMed: 10357476]

45. Kuehne T, Saeed M, Higgins CB, Gleason K, Krombach GA, Weber OM, Martin AJ, Turner D, Teitel D, Moore P. Endovascular stents in pulmonary valve and artery in swine: feasibility study of MR imaging-guided deployment and postinterventional assessment. Radiology Feb;2003 226(2):475–481. [PubMed: 12563142]

Figure 1.
Custom active CTO guidewire telescoped within custom active CTO support catheter.

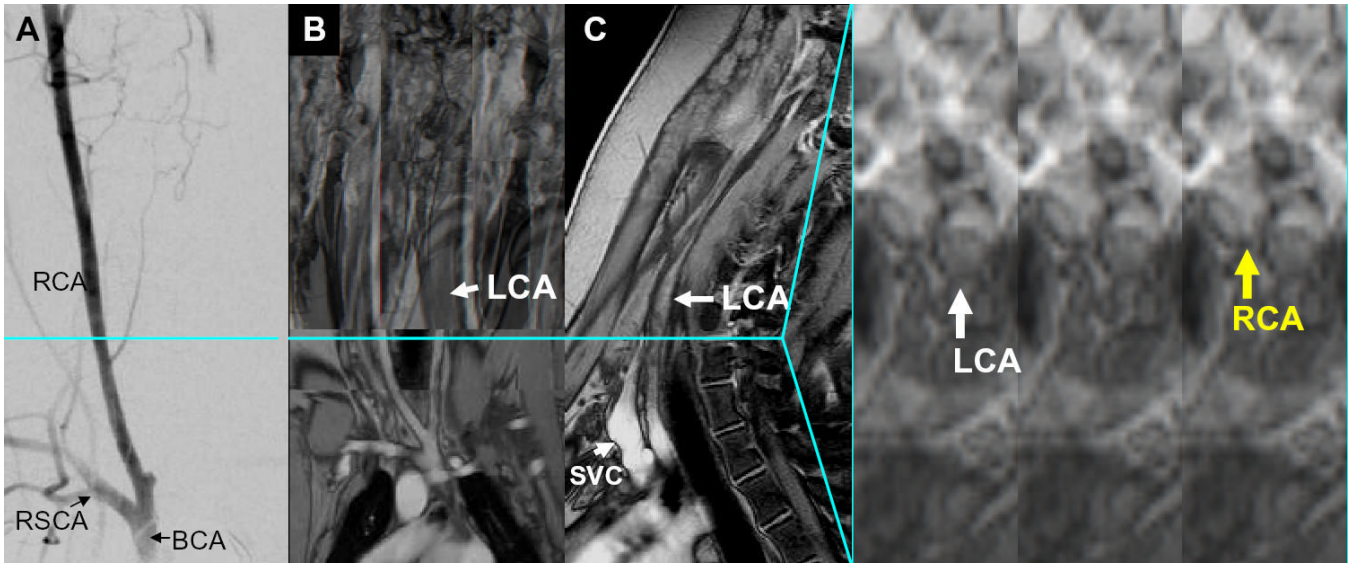

Figure 2.
Baseline imaging of CTO lesions. (A) AP projection subtraction X-ray demonstrating "invisible" long LCA occlusion with distal reconstitution. Multislice T1 weighted spin echo composite clearly demonstrates the entire occluded LCA in the (B) coronal, (C) sagittal, and (D) axial views. Linear dissection in the LCA is evident in the axial slice at this level (blue line). LCA = left carotid artery, RCA = right carotid artery, RSCA = right subclavian artery, BCA = brachiocephalic artery, SVC = superior vena cava

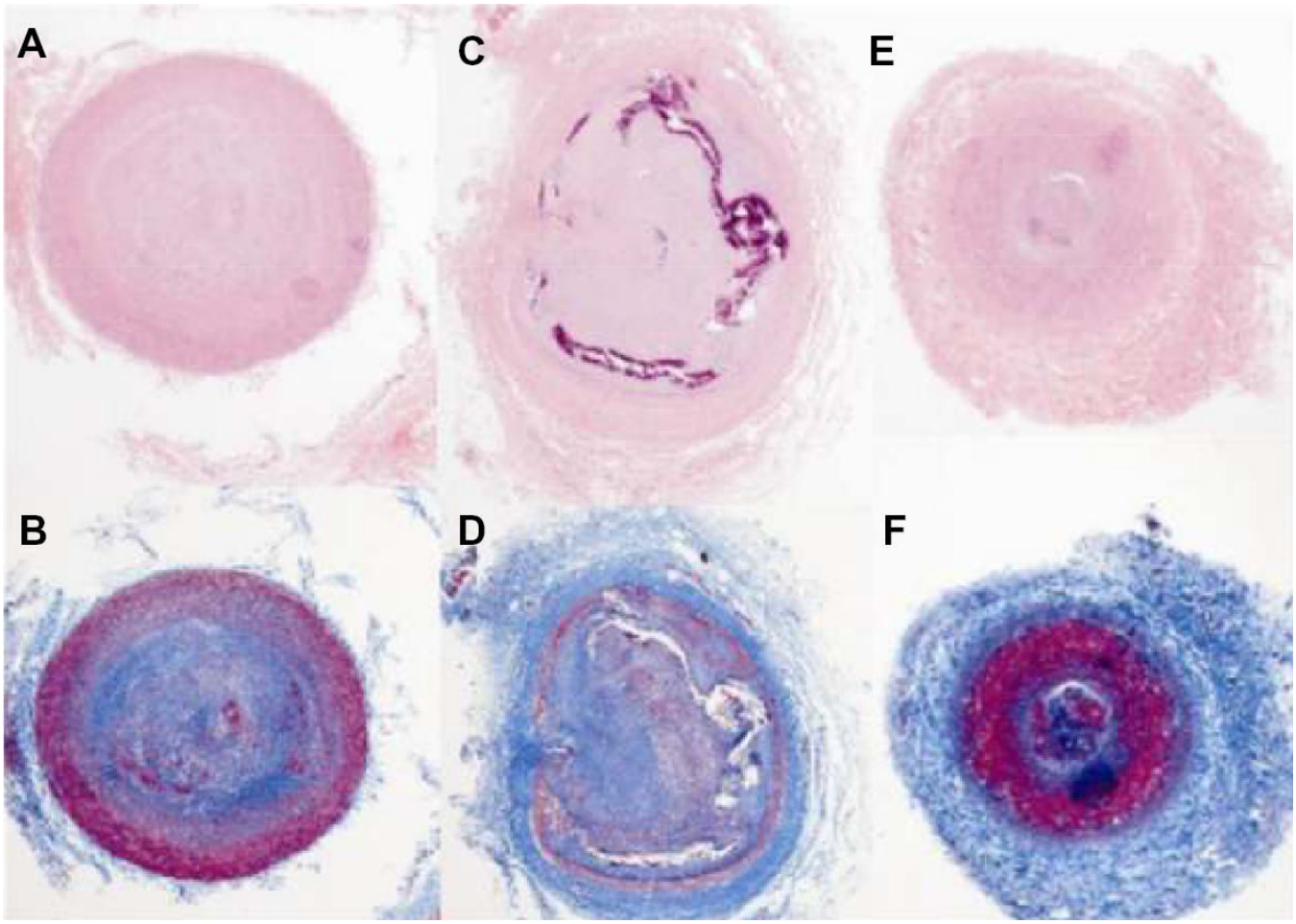

Figure 3.
Representative histopathology sections, 4X magnification. (A–B)Proximal, (C–D)mid, and (E–F)distal transverse sections of CTO artery stained with Hematoxylin and Eosin (H&E) (top row) and Trichrome (bottom row). The central lumen is filled with collagen (pink in A, C, E, blue in B,D,F), disrupted intima with cellular infiltration (purple in C) and indispersed microchannels (C,D). Distal section approximately 80cm distal to bifurcation has intact intima and organized thrombus (red in F).

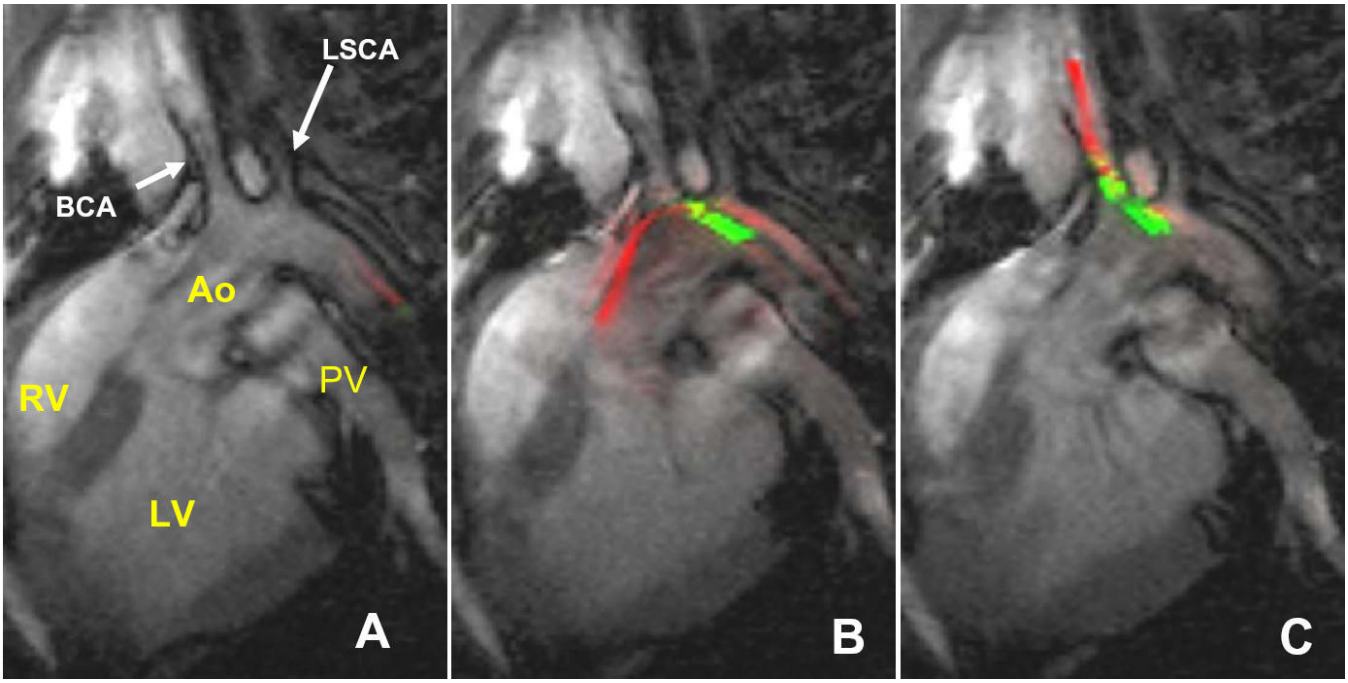

Figure 4.
Positioning devices under rtMRI to begin CTO attempt. (A) Active wire (red) entering descending aortic arch (Ao). (B)The leading active wire positioned safely in ascending aorta (Ao), and the active catheter (green) follows. (C)Active wire and subsequently catheter are easily steered into brachiocephalic artery. RV = right ventricle. LV = left ventricle, PV = pulmonary vein.

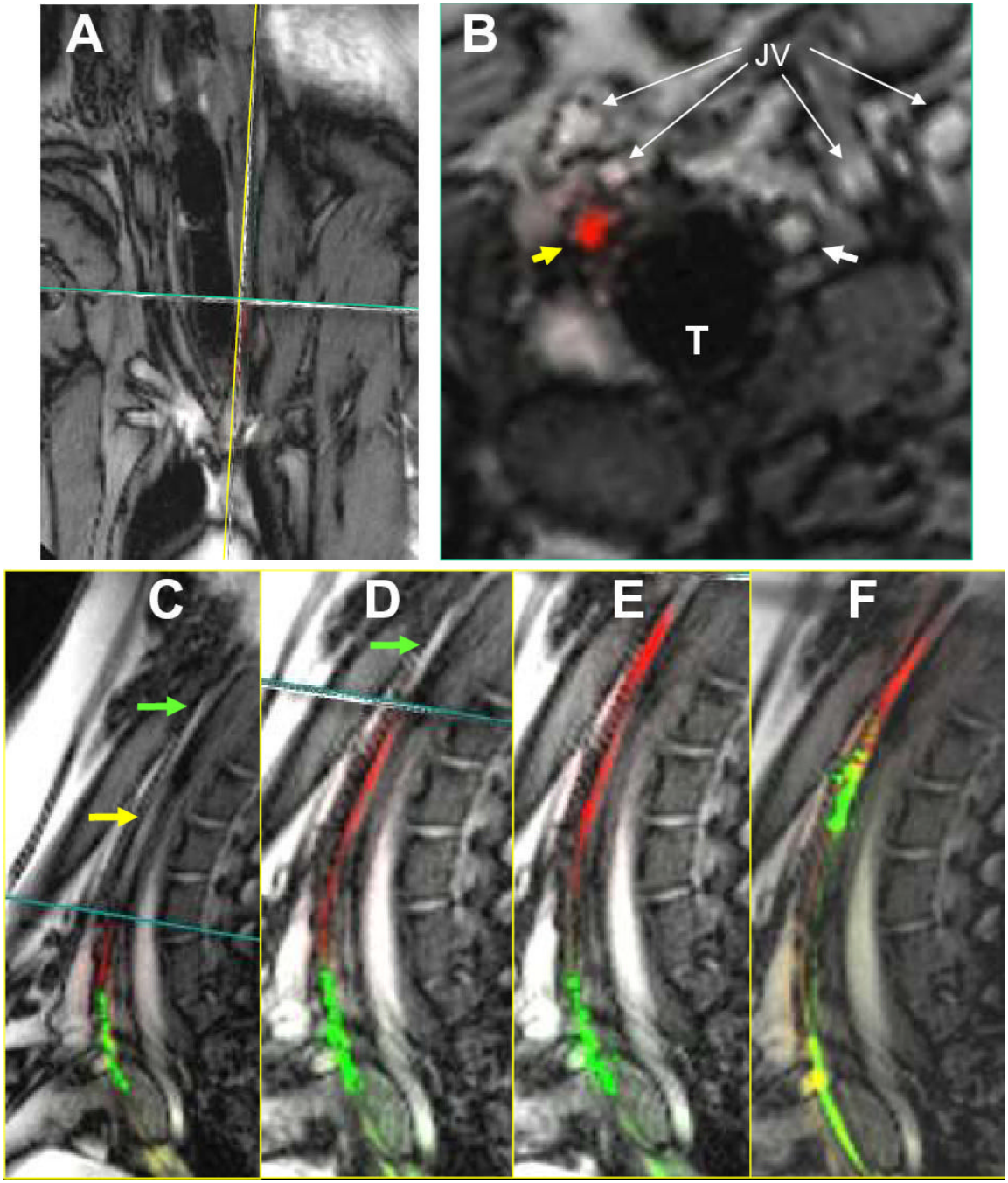

Figure 5.
Traversing CTO with active guidewire and catheter. (A)Real-time, interleaved, multiplanar MRI of coronal, sagittal and transverse slices through occluded LCA. (B)Transverse slice demonstrates RCA (white arrow) and occluded LCA (yellow arrow). The active CTO wire tip (red) is seen entirely within the LCA lumen. (C) Sagittal view of the occluded LCA (yellow arrow). The active wire (red) and catheter (green) are visualized proximally in the occluded LCA. The transverse slice (B) is continually translated cranially in advance of the CTO wire tip. (D) The active wire is advanced through the remaining CTO into the patent distal LCA. (E) The active catheter is tracked over the fixed wire into the distal patent LCA. (F) 5x100mm angioplasty balloon inflated with dilute Gd-DTPA over active delivery wire (green). LCA =

left carotid artery, RCA = right carotid artery, T = trachea, JV = external and internal jugular veins.

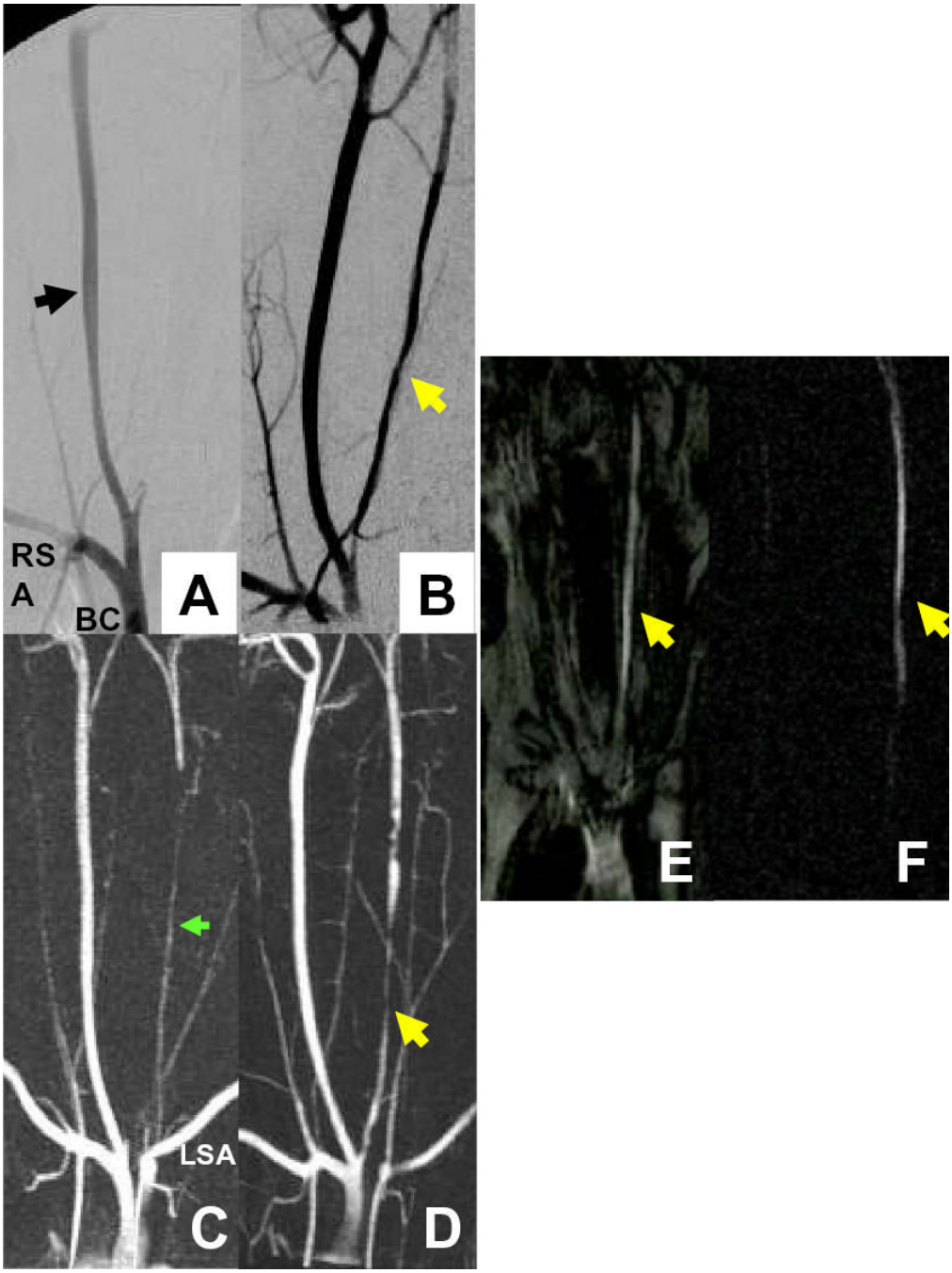

Figure 6.

Multimodal angiography before and after CTO recanalization. (A,B) Pre and post intervention AP projection subtraction X-ray demonstrates right carotid artery (black arrow) and patent post-intervention left carotid artery (LCA) CTO (yellow arrow). (C,D) Pre and post intervention CEMRA in the AP projection. Pre-intervention, the distal artery reconstitutes via cerebral collateral circulation with contribution from the left verterbral artery (green arrow) arising from the left subclavian artery (LSA). (E,F) Selective real-time angiography gives immediate confirmation of successful recanalization into the patent LCA (yellow arrows) with saturation prepulse applied (E) and with better contrast with subtraction maximal intensity-over-time projection (F) . AP = antero-posterior, CEMRA = contrast enhanced MRA

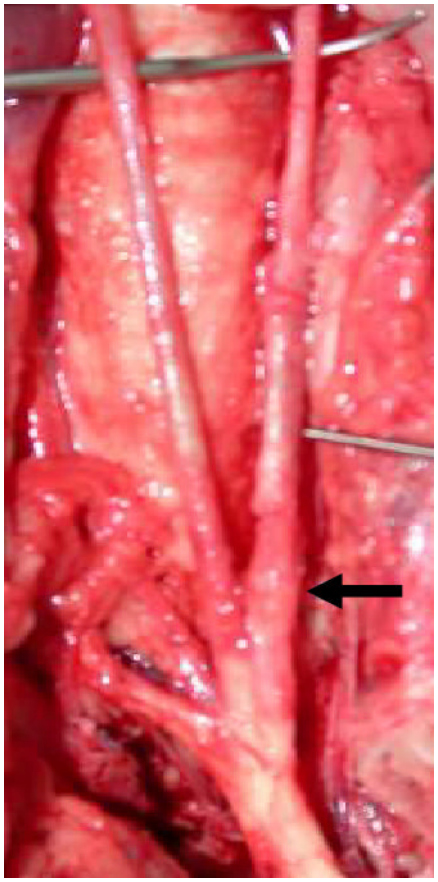

Figure 7.
Gross necropsy of a successfully recanalized CTO demonstrates proximal left carotid artery thickening (black arrow) with no extramural injury.